

Liver-directed *SERPINA1* gene therapy attenuates progression of spontaneous and tobacco smoke-induced emphysema in α_1 -antitrypsin null mice

Marina Zieger,^{1,3} Florie Borel,^{1,3} Cynthia Greer,¹ Gwladys Gernoux,^{1,2} Meghan Blackwood,¹ Terence R. Flotte,^{1,2} and Christian Mueller^{1,2,3}

¹The Li Weibo Institute for Rare Diseases Research, Horae Gene Therapy Center, 368 Plantation Street, Worcester, MA 01605, USA; ²Department of Pediatrics, University of Massachusetts Chan Medical School, 368 Plantation Street, Worcester, MA 01605, USA

α_1 -antitrypsin deficiency is a rare genetic condition that can cause liver and/or lung disease. There is currently no cure for this disorder, although repeated infusions of plasma-purified protein may slow down emphysema progression. Gene therapy in which a single recombinant adeno-associated viral vector (rAAV) administration would lead to sustained protein expression could therefore similarly affect disease progression, and provide the added benefits of reducing treatment burden and thereby improving the patient's quality of life. The study presented here tests whether treating the *Serpina1a-e* knockout mouse model of α_1 -antitrypsin-deficiency lung disease with gene therapy would have an impact on the disease course, either on spontaneous disease caused by aging or on accelerated disease caused by exposure to cigarette smoke. Liver-directed gene therapy led to dose-dependent levels of biologically active human α_1 -antitrypsin protein. Furthermore, decreased lung compliance and increased elastic recoil indicate that treated mice had largely preserved lung tissue elasticity and alveolar wall integrity compared with untreated mice. rAAV-mediated gene augmentation is therefore able to compensate for the loss of function and restore a beneficial lung protease-antiprotease balance. This work constitutes a preclinical study report of a disease-modifying treatment in the *Serpina1a-e* knockout mouse model using a liver-specific rAAV serotype 8 capsid.

INTRODUCTION

Emphysema is a major life-limiting chronic obstructive pulmonary disease (COPD) condition, and the leading genetic cause of it is a monogenic disease, α_1 -antitrypsin deficiency (AATD).^{1–4} AATD is an autosomal codominant disorder caused by variants in the *SERPINA1* gene encoding serine protease inhibitor α_1 -antitrypsin (AAT) protein. AATD has been recognized in all populations worldwide.⁵ However, it is a largely underdiagnosed monogenic condition, and less than 10% of severely deficient individuals are currently identified.^{6–8}

Over 80% of AAT is synthesized and secreted by hepatocytes, and 0.5%–10% reaches the alveolar fluid from plasma, with local concentrations ranging from 100 to 300 $\mu\text{g/mL}$.⁹ The normal range of circulating AAT protein level is estimated to be 20 to 53 μM (1,000 to

2,000 $\mu\text{g/mL}$). Based on genotype-phenotype studies, it is estimated that plasma levels below the serum protective threshold of 11 μM (572 $\mu\text{g/mL}$) significantly increase the risk of developing lung emphysema.¹⁰

Low levels of circulating AAT have been found to result in excessive cleavage of extracellular and cell-surface proteins in the alveolar epithelium by a number of proteolytic enzymes, including neutrophil elastase, proteinase 3, cathepsin G, and neutrophil serine protease 4, released from activated neutrophils.^{11–17} AAT is also antiapoptotic in pulmonary endothelial cells, primarily via the inhibition of caspase-3.^{18,19}

AAT functions to irreversibly inactivate excess free serine proteinase elastase released by neutrophils during inflammation caused by respiratory infections, air pollutants, and cigarette smoke, thus protecting the alveolar interstitium and capillary bed from degradation and enabling regeneration of the pulmonary parenchyma.^{20–22} AAT deficiency is further exacerbated clinically through oxidant-mediated inactivation in the context of tobacco smoke exposure.²³

Emphysema is characterized by destruction of the interalveolar septa, loss of capillaries, reduced lung elastic recoil, and diminished lung diffusion capacity and, as a result, life-threatening respiratory insufficiency in human patients. AATD subjects can suffer from liver disease of varying severity at a very young age; however, lung disease is the principal cause of mortality among elderly subjects.^{4,8,24}

Currently there is no cure for AATD. Although AAT protein augmentation therapy is safe and effective at slowing emphysema

Received 31 July 2021; accepted 10 April 2022;
<https://doi.org/10.1016/j.omtm.2022.04.003>.

³Present address: Apic Bio, Inc., 35 Cambridgepark Dr, Suite 350, Cambridge, MA 02140, USA

Correspondence: Christian Mueller, The Li Weibo Institute for Rare Diseases Research, Horae Gene Therapy Center, 368 Plantation Street, Worcester, MA 01605, USA.

E-mail: christian.mueller4@sanofi.com



progression in AAT-deficient patients, it requires costly weekly intravenous infusions of pooled human donor plasma in order to maintain sufficiently high levels of AAT protein in serum and lung epithelial-lining fluid.²⁵

In contrast, gene therapy may offer treatment of AATD following a one-time administration of a recombinant adeno-associated viral vector (rAAV) that mediates *SERPINA1* gene delivery and long-term AAT expression.^{26,27} Several studies have established proof of concept in animal models through liver-directed,^{28–30} muscle-directed,^{31–33} or lung-directed routes.^{34–37}

In this study we demonstrate the therapeutic efficacy of liver-directed, rAAV-mediated delivery of the human *SERPINA1* gene for emphysema therapy. We used the *Serpina1a-e Null* (hereafter “knockout”) mouse generated in our laboratory as a model of spontaneous and cigarette smoke-aggravated genetic emphysema. Due to the absence of endogenous mouse AAT protein, these mice closely recapitulate the specific clinical characteristics of bilateral panacinar emphysema found in AAT null patients.^{38,39} We provide here evidence of therapeutic gene augmentation that compensates for the loss of AAT function through restored protease-antiprotease balance *in vivo*.

RESULTS

Aged *Serpina1a-e* knockout mice spontaneously develop an emphysema phenotype

To determine a therapeutic window, aged *Serpina1a-e* knockout mice were examined for pulmonary phenotype at the ages of 18, 28, and 52 weeks, and the averages of three maneuvers per mouse were compared with those of age-matched wild-type mice. The upward shift of pressure-volume loops showed that the lung volumes of *Serpina1a-e* knockout mice continuously increased from 0.59 ± 0.07 to 0.64 ± 0.08 to 0.70 ± 0.08 mL, while 52-week-old wild-type mice reached a maximum lung volume of 0.63 ± 0.07 mL (Figures 1A and 1B). Accordingly, lung compliance significantly increased from 0.084 ± 0.002 mL/H₂O in 18-week-old and 0.089 ± 0.002 mL/H₂O in 28-week-old to 0.10 ± 0.003 mL/H₂O in 52-week-old knockouts, compared with 18-week-old (0.075 ± 0.002 mL/H₂O), 28-week-old (0.081 ± 0.002 mL/H₂O), and 52-week-old (0.082 ± 0.002 mL/H₂O) wild-type mice (Figure 1C). Importantly, tissue elastance decreased from 20.55 ± 0.48 cm/H₂O/s/mL in 18-week-old and 18.82 ± 0.61 cm/H₂O/s/mL in 28-week-old to 15.28 ± 0.26 cm/H₂O/s/mL in 52-week-old knockout mice, while no significant change was observed in wild-type mice between 28 and 52 weeks of age (22.55 ± 0.59 , 19.85 ± 0.46 , 19.00 ± 0.52 cm/H₂O/s/mL) (Figure 1D). Destruction of the alveolar walls followed by degradation of the lung parenchyma may hypothetically be causing the observed overinflation of the lung. We therefore measured alveolar air spaces in lung sections (Figure 1E). The enlargement of alveolar spaces was evident from the decreased probability density in the healthy alveolar diameter range (20–40 μm) and corresponding increased probability density in the damaged range (50–80 μm) in *Serpina1a-e* knockout mice of all three age groups, compared with age-matched wild-type mice (Figures 1F and S1A–A1C). Overall, these results point to an early onset of a slowly

progressing lung emphysema phenotype in *Serpina1a-e* knockout mice. Moreover, the observed decline in pulmonary function and enlargement of alveolar air spaces in knockout mice are associated with a decrease in lung parenchyma elastic recoil, which influences emphysema disease severity.

rAAV-mediated expression of *SERPINA1* produces therapeutic levels of biologically active α_1 -proteinase inhibitor and protects *Serpina1a-e Null* mice from emphysema

To test treatment efficacy, *Serpina1a-e* knockout mice were treated as young adults and followed up longitudinally. An rAAV vector expressing wild-type human AAT (hAAT) (Figure 2A) was systemically injected into 16-week-old knockout mice at two different doses (1.4×10^{11} and 5.0×10^{10} genome copies [gc]/mouse), and the animals were subsequently followed for 36 weeks (Figure 2B). At study end, pulmonary mechanics were assessed and three maneuvers per mouse were averaged. Lung volumes of rAAV-treated knockout mice (0.64 ± 0.08 and 0.66 ± 0.08 mL for the 1.4×10^{11} and 5.0×10^{10} gc doses, respectively) were comparable to that of wild-type controls (0.63 ± 0.07 mL) but differed from that of vehicle-treated knockouts (0.72 ± 0.08 mL) (Figures 2C and 2D). Lung compliance was significantly decreased in rAAV-treated knockouts (0.091 ± 0.002 and 0.094 ± 0.002 mL/H₂O for the 1.4×10^{11} and 5.0×10^{10} gc doses, respectively) as compared with vehicle-treated mice (0.10 ± 0.002 mL/H₂O) and was comparable to that of wild-type controls (0.088 ± 0.002 mL/H₂O) (Figure 2E). Tissue elastance was significantly preserved in mice treated with 1.4×10^{11} gc (16.77 ± 0.74 cm/H₂O/s/mL) compared with wild-type controls (18.16 ± 0.52 cm/H₂O/s/mL), while mice treated with 5.0×10^{10} gc showed no improvement and retained a tissue elastance (15.65 ± 0.38 cm/H₂O/s/mL) comparable to that measured in vehicle-treated mice (15.03 ± 0.25 cm/H₂O/s/mL, Figure 2F). rAAV treatment produced levels of hAAT that were stable over the duration of the study ($\sim 3,000$ μg/mL (~ 58 μM) at high dose and $\sim 1,000$ μg/mL (~ 19 μM) at low dose as measured at the endpoint, Figure 2G); quantification of the protein biological activity against human elastase indicated that the secreted hAAT protein was biochemically active and could effectively inhibit neutrophil elastase (Figure 2H). Cellular analysis of bronchoalveolar lavage cytopins reflected an unchanged presence of lymphocytes in vehicle-treated ($21.0\% \pm 4.8\%$ and $20.8\% \pm 1.8\%$) and in rAAV-treated ($11.6\% \pm 2.2\%$ and $11.2\% \pm 1.9\%$) knockout mice. However, significantly increased presence of neutrophils ($18.1\% \pm 1.4\%$) was evident in vehicle-treated knockouts ($n = 3$) compared with ($7.0\% \pm 0.8\%$) wild-type controls, whereas a significantly reduced influx of neutrophils, $3.3\% \pm 1.0\%$ and $2.7\% \pm 0.9\%$, was measured in the rAAV-treated knockouts at 1.4×10^{11} and 5.0×10^{10} gc dose, respectively (Figure 2I). Finally, we measured lung air spaces in rAAV-treated and vehicle-treated knockout mice. An increased probability density in the healthy alveolar diameter range (20–30 μm) and decreased probability density in the damaged alveolar diameter range (50–70 μm) were observed in rAAV-treated mice compared with vehicle-treated controls (Figures 3A and 3B), demonstrating preservation of the interalveolar septa.

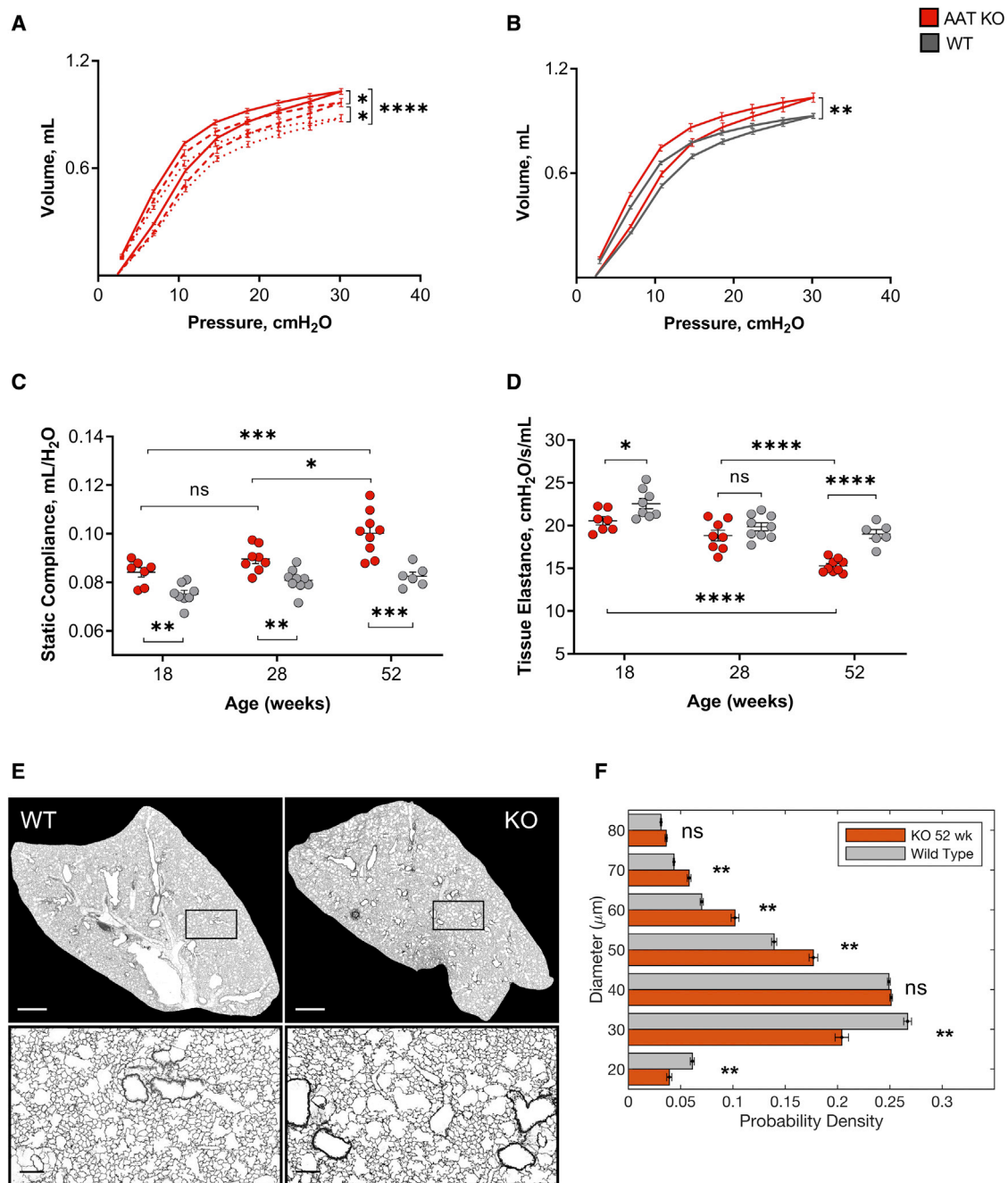


Figure 1. Aged *Serpina1a-e* knockout mice spontaneously develop an emphysema phenotype

Key respiratory parameters were assessed in knockout and age-matched wild-type mice. Averages of three maneuvers per mouse are shown, along with the age group mean. (A and B) Pressure-volume (PV) loops (red dotted line, 18-week-old knockouts, n = 7; red dashed line, 28-week-old knockouts, n = 8; red solid line, 52-week-old knockouts, n = 9; gray solid line, 52-week-old wild-type control, n = 6). (C) Static compliance and (D) tissue elastance (red circle, knockout mice; gray circle, age-matched wild-type control mice). Histological changes were assessed in fixed lung sections. (E) Representative segmented images of left lung lobe showing airway and alveolar boundaries (black contour line) (52-week-old wild-type mouse (left top and bottom) and age-matched knockout mouse (right top and bottom)) (see also [Materials and methods](#)). (F) Histogram of distribution, showing the decreased probability density in the healthy alveolar diameter range (20–40 μm) and increased probability density in the damaged range (50–80 μm) in 52-week-old knockout mice (red bar) compared with control, wild-type mice (gray bar) (n = 5 wild type; n = 7 knockout). Shift of PV loops upward (in A), increased lung compliance, and decreased elastic recoil are due to destruction of alveolar walls (in E, right) followed by degradation of lung parenchyma that is causing overinflation of the lung. Error bars represent the SEM. Statistical significance was determined by two-tailed unpaired t test, except for the PV loops (two-way ANOVA). ns, p > 0.05; *p ≤ 0.05; **p ≤ 0.01; ***p ≤ 0.001; ****p ≤ 0.0001. Scale bars, 1 mm (top), 150 μm (bottom).

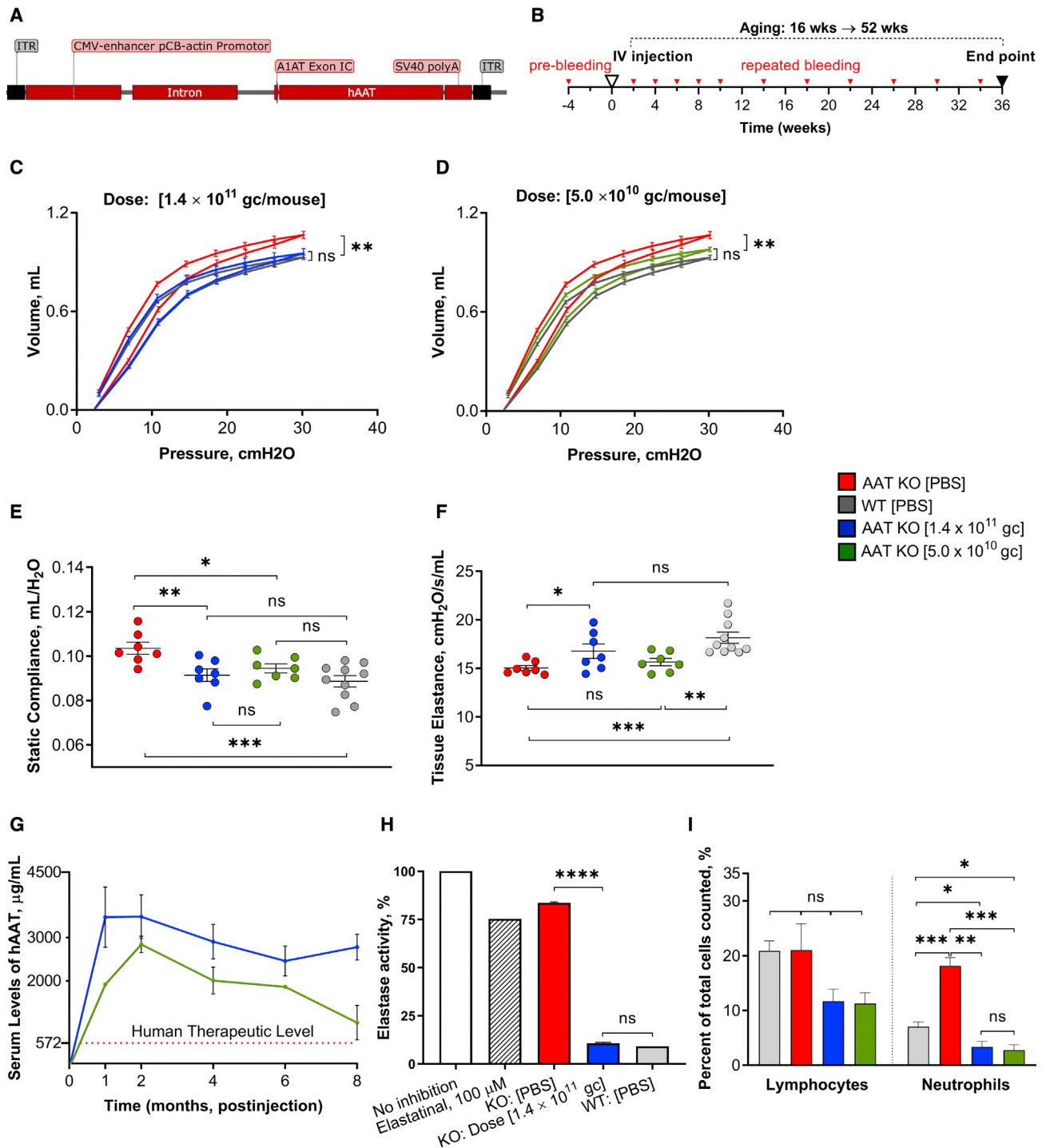


Figure 2. rAAV-mediated *SERPINA1* transgene expression produces therapeutic levels of biologically active α_1 -proteinase inhibitor and preserves pulmonary function in aged *Serpina1a-e* knockout mice

(A) Schematic of the single-function pCB-hAAT vector construct. The expression cassettes contain a single-stranded DNA molecule with AAV serotype 2 inverted terminal repeats (ITRs) flanking a gene cassette comprising cytomegalovirus immediate-early enhancer/chicken β -actin hybrid promoter sequences, cDNA encoding wild-type human α_1 -antitrypsin (AAT) with exon 1C, and an SV40 polyadenylation signal. The expression cassette was packaged in the liver-specific AAV serotype 8 capsid. (B) Schematic showing the experimental design: the rAAV-hAAT single-function vector was systemically infused by a single tail vein injection at two different doses into the livers of 16-week-old knockout mice, and the animals were subsequently followed for 36 weeks. Mouse serum was collected to measure levels of human AAT by ELISA at various

(legend continued on next page)

Cigarette smoke exposure accelerates emphysema development in young adult *Serpina1 a-e* knockout mice

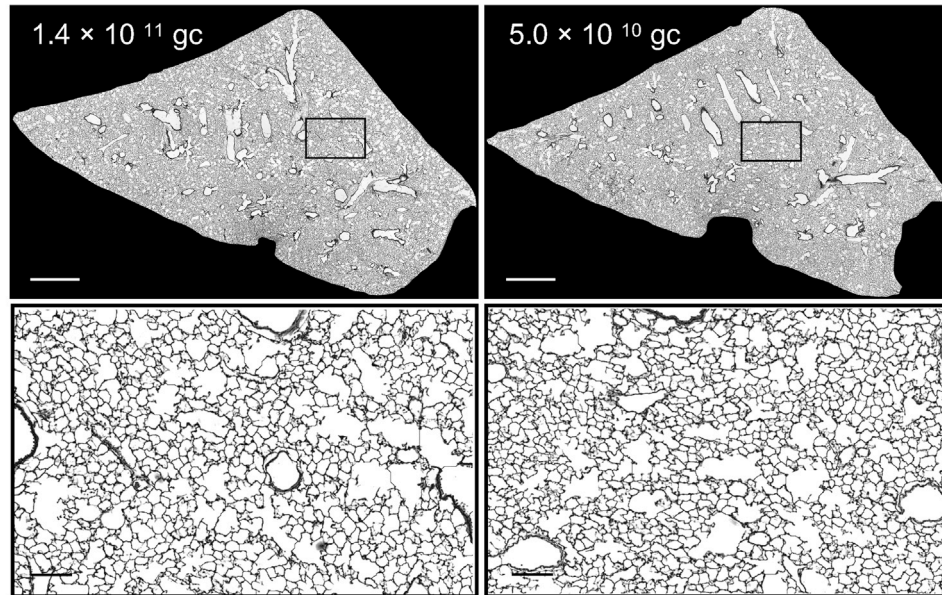
Young adult (10 weeks old) knockout and wild-type mice were whole-body exposed to cigarette smoke for a period of 8 weeks (Figure 4A) to accelerate the emphysema phenotype development. In the whole-body exposure chamber, cigarette smoke can be absorbed through the skin and the gastrointestinal tract. Cotinine, the primary metabolite of nicotine, was therefore used as a biomarker of exposure to toxic tobacco agents. At baseline (room air), serum levels of cotinine in knockout and wild-type animals were similar (0.54 ± 0.48 and 0.35 ± 0.18 ng/mL, respectively). Exposure to four cigarettes for 20 min produced comparable serum levels of cotinine in wild-type (5.0 ± 0.3 ng/mL) and knockout mice (5.6 ± 0.6 ng/mL), as measured by anti-mouse soluble cotinine ELISA (Figure 4B). Pulmonary mechanics were assessed in age-matched knockouts and wild-type mice exposed to either cigarette smoke or room air. An upward shift of pressure-volume loops was observed in the knockouts exposed to cigarette smoke (0.59 ± 0.07 mL) as opposed to room air (0.68 ± 0.08 mL, Figure 4C), as well as increased compliance (from 0.082 ± 0.002 to 0.10 ± 0.002 mL/H₂O, Figure 4D) and decreased tissue elastance (from 19.89 ± 0.50 to 18.00 ± 0.42 cm/H₂O/s/mL, Figure 4E). There were no changes in lung volumes (0.54 ± 0.07 mL versus 0.52 ± 0.06 mL), compliance (0.074 ± 0.002 mL/H₂O versus 0.74 ± 0.003 mL/H₂O) or tissue elastance (23.31 ± 0.78 cm/H₂O/s/mL versus 23.26 ± 0.68 cm/H₂O/s/mL) in cigarette smoke-exposed versus room air-exposed wild-type mice (Figures 4C–4E). Profound damage to the lung microarchitecture was observed in cigarette smoke-exposed knockout mice (Figures 4F–4H). Probability density of alveolar spaces in the healthy alveolar diameter range (20–40 μm) was significantly decreased, and a respective increase in enlarged alveolar spaces (70 μm) was evident in cigarette smoke-exposed knockout mice compared with room air-exposed knockout mice (Figure 4I). No changes in alveolar spaces were measured in wild-type mice in response to exposure (Figure 4J). Therefore, the proposed regimen of cigarette smoke exposure induced the aggravated destruction of alveolar walls and resulted in the accelerated decline of lung function in *Serpina1a-e* knockout mice, but not in wild-type mice, which tolerated it well.

rAAV-mediated expression of *SERPINA1* protects lung parenchyma and preserves pulmonary function in *Serpina1a-e* knockout mice exposed to cigarette smoke

rAAV-hAAT was systemically injected into 12-week-old knockout mice at two different doses (5.0×10^{10} and 2.9×10^{11} gc/mouse, Figure 5A). Two weeks post-treatment, the mice were exposed to cigarette smoke for a period of 8 weeks (Figure 5B), after which pulmonary mechanics were assessed. At both doses, rAAV-treated knockout mice demonstrated decreased lung volumes (0.60 ± 0.07 and 0.61 ± 0.07 mL compared with 0.68 ± 0.08 mL in vehicle-treated knockouts, Figures 5C and S2A), decreased lung compliance (0.085 ± 0.003 and 0.086 ± 0.002 mL/H₂O compared with 0.096 ± 0.002 mL/H₂O in vehicle-treated knockouts, Figures 5D and S2B), and increased elastic recoil (19.78 ± 0.61 and 20.63 ± 0.45 cm/H₂O/s/mL compared with 17.60 ± 0.36 cm/H₂O/s/mL in vehicle-treated knockouts, Figures 5E and S2C). The significantly improved lung function indicates that rAAV-AAT treatment helped to preserve the elastic properties of lung tissue and the integrity of alveolar walls compared with untreated AAT knockout control mice. Accordingly, protection of the alveolar septa was evident from increased probability density in the healthy alveolar diameter range (30–40 μm) and decreased probability density in the damaged alveolar diameter range (60 μm) in rAAV-treated *Serpina1a-e* knockout mice exposed to cigarette smoke compared with vehicle-treated control mice (Figures 5F–5H, S2D, and S2E). Serum hAAT protein reached levels of $\sim 3,000$ μg/mL (~ 58 μM) at the 5.0×10^{10} gc/mouse dose and $10,000$ μg/mL ($\sim 2,100$ μM) at the 2.9×10^{11} gc/mouse dose (Figures 5I and S2F). At the baseline, under room air exposure, bronchoalveolar lavage differential cell counts in 22-week-old knockouts were comparable to the corresponding cell counts found in age-matched wild-type mice ($4.6\% \pm 0.7\%$ and $4.6\% \pm 0.9\%$ for lymphocytes, $0.67\% \pm 0.33\%$ and $0.83\% \pm 0.60\%$ for neutrophils, respectively). In contrast, cellular analysis demonstrated increased inflammatory cell profiles of both lymphocytes ($7.6\% \pm 0.7\%$) and neutrophils ($2.90\% \pm 0.58\%$) in cigarette smoke-challenged knockouts compared with knockouts exposed to room air. The lavage cellular counts did not change significantly in smoke- compared with room air-exposed wild-type mice. Remarkably, both the lymphocyte and the

time points (red triangles) (see also Materials and methods). Key respiratory parameters were assessed in rAAV-injected mice and compared with vehicle-treated age-matched control knockout and wild-type mice at 52 weeks of age. Averages of three maneuvers per mouse are shown, along with the age group mean. (C and D) Pressure-volume (PV) loops (red line, vehicle-treated knockouts, $n = 7$; blue line [C], knockouts injected at 1.4×10^{11} vector genome copies per mouse [gc/mouse], $n = 7$; green line [D], knockouts injected at 5.0×10^{10} gc/mouse, $n = 7$; gray line, untreated wild-type control, $n = 10$). (E) Static compliance and (F) tissue elastance (red circle, vehicle-treated knockout; blue circle, knockout dosed at 1.4×10^{11} gc/mouse; green circle, knockout dosed at 5.0×10^{10} gc/mouse; gray circle, wild-type control). Shift of PV loops downward (in C and D), decreased lung compliance (in E), and increased elastic recoil (in F) indicate that mice expressing human AAT largely preserve the elastic properties of the lung tissue compared with vehicle-treated knockout mice. (G) Single-function vector generated high-level transgene expression to produce significant, stable over time, systemic levels of human AAT protein (blue line, knockouts dosed at 1.4×10^{11} gc/mouse, $\sim 3,000$ μg/mL at the endpoint; green line, knockouts dosed at 5.0×10^{10} gc/mouse, $\sim 1,000$ μg/mL at the endpoint; $n = 3$ per each dosed group). Mouse livers secreted fully biochemically active AAT proteinase inhibitor protein. (H) Biological activity of AAT against human neutrophil elastase was measured by human neutrophil elastase activity (NEA) assay *in vitro* (vehicle-treated, $n = 7$, and rAAV-treated knockouts, $n = 8$, with expression of human AAT at $\sim 2,000$ μg/mL). (I) Cellular analysis of bronchoalveolar lavage cytopspins reflects unchanged presence of lymphocytes (left) and increased presence of neutrophils (right) in aged vehicle-treated knockout mice (red bars) compared with wild-type controls (gray bars), while significantly reduced influx of neutrophils was evident in rAAV-treated (blue bars, knockouts dosed at 1.4×10^{11} gc/mouse; green bars, knockouts dosed at 5.0×10^{10} gc/mouse) endpoint mouse lung air spaces ($n = 3$ per group). Error bars represent the SEM. Statistical significance was determined either by two-tailed unpaired t test or the Holm-Šidák method (for cellular analysis), with $\alpha = 0.05$, except for the PV loops (two-way ANOVA). ns, $p > 0.05$; * $p \leq 0.05$; ** $p \leq 0.01$; *** $p \leq 0.001$; **** $p \leq 0.0001$.

A



B

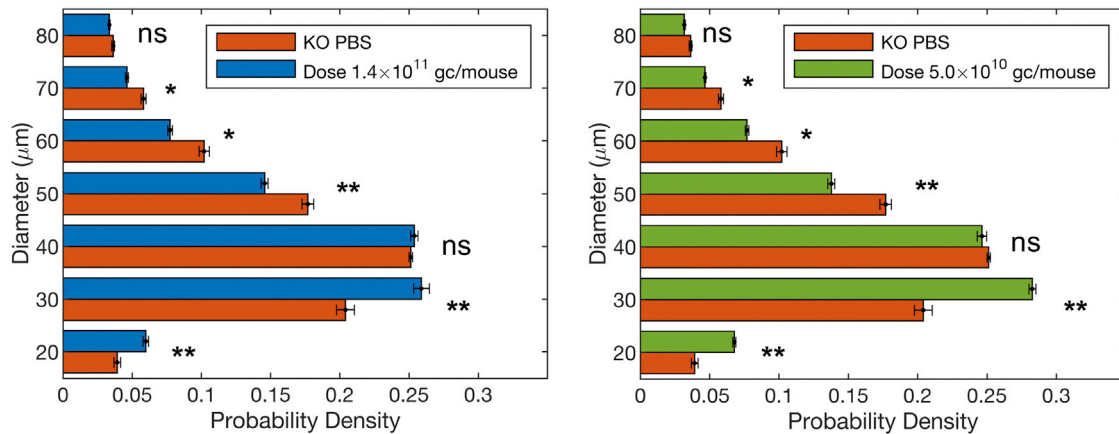


Figure 3. rAAV-mediated *SERPINA1* transgene expression protects alveolar wall integrity in *Serpina1a-e* knockout mice

Histological changes were assessed in fixed lung sections. (A) Representative segmented images of left lung lobe showing airway and alveolar boundaries (black contour line) in knockouts dosed at 1.4×10^{11} gc/mouse (left top and bottom) and knockouts dosed at 5.0×10^{10} gc/mouse (right top and bottom) (see also [Materials and methods](#)). (B) Histograms of distribution, showing the increased probability density in the healthy alveolar diameter range (20–40 μm) and decreased probability density in the damaged range (50–80 μm) in knockout mice treated with rAAV at 1.4×10^{11} gc (blue bars, left, $n = 6$) or rAAV at 5.0×10^{10} gc (green bars, right, $n = 4$), compared with vehicle-treated knockout mice (red bars, $n = 7$). Error bars represent the SEM. Statistical significance was determined by two-tailed unpaired t test. ns, $p > 0.05$; * $p \leq 0.05$; ** $p \leq 0.01$. Scale bars, 1 mm (top), 150 μm (bottom).

neutrophil counts were significantly reduced ($3.33\% \pm 0.88\%$ and $0.5\% \pm 0.1\%$, respectively) in cigarette smoke-exposed knockout mice treated with 5.0×10^{10} gc/mouse dose of vector and were close to counts found in cigarette smoke-exposed wild-type mice ($3.00\% \pm 0.80\%$ and $0.50\% \pm 0.10\%$, respectively) (Figure 5J). Neither lymphocyte nor neutrophil counts were significantly changed in knockout mice treated with 2.9×10^{11} gc compared with control knockout and wild-type mouse groups (Figure S2G).

DISCUSSION

Emphysema is a condition that is anatomically characterized by abnormal enlargement of the alveolar spaces resulting in loss of lung elastic recoil. We previously described the generation of the *Serpina1a-e* knockout model and showed that this mouse had undetectable levels of murine AAT and developed spontaneous emphysema, making this model highly relevant not only to the preclinical development of therapeutics for AATD, but also to research on smoking-related

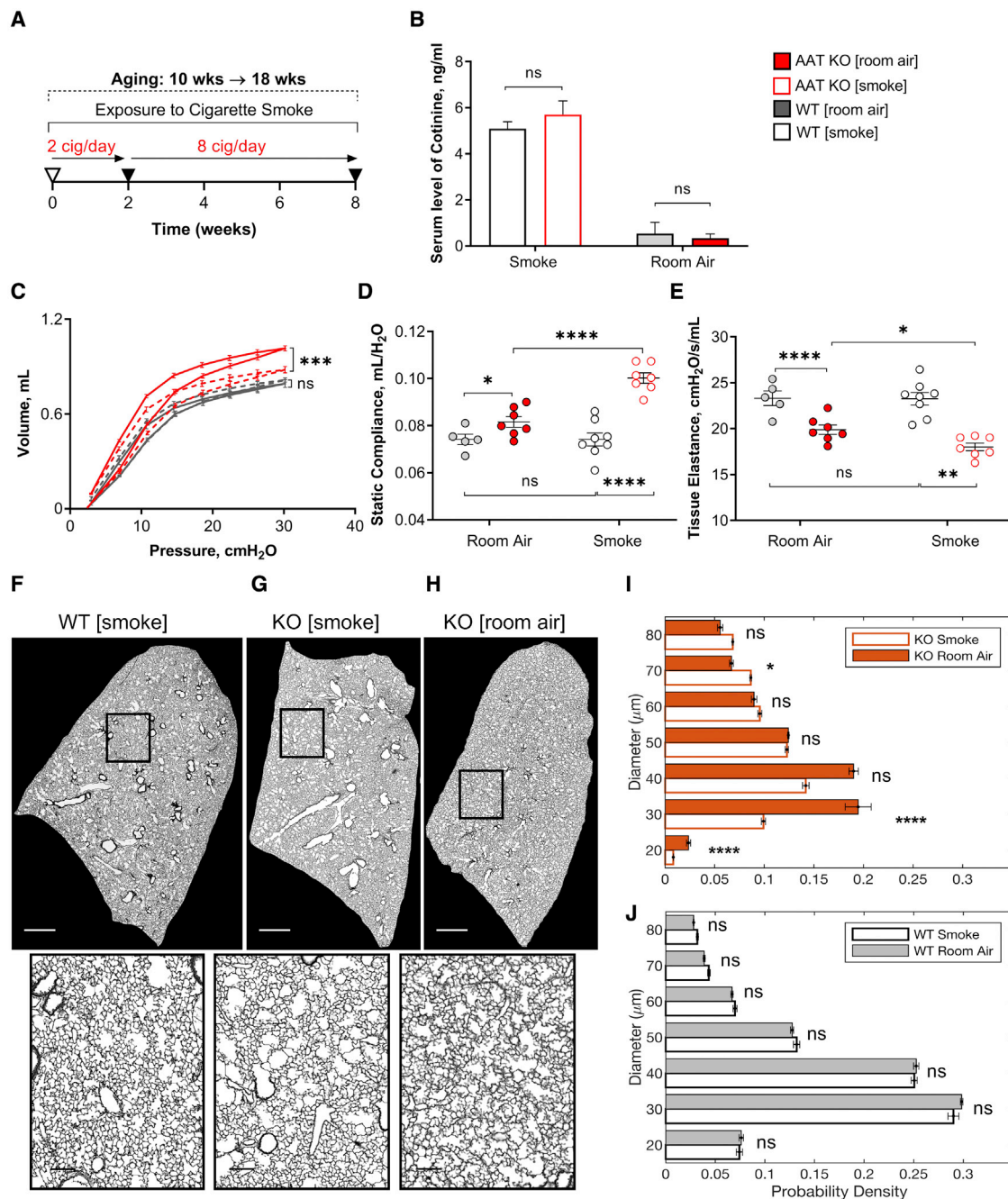


Figure 4. Cigarette smoke exposure accelerates emphysema development in young adult *Serpina1a-e* knockout mice

(A) Schematic showing the experimental design: 10-week-old knockout and wild-type mice were whole-body exposed to cigarette smoke for 8 weeks (see [Materials and methods](#)). The level of systemic exposure was assessed in knockout and wild-type mice. (B) Exposure to four cigarettes for 20 min produced comparable serum levels of nicotine metabolite cotinine in wild-type and knockout mice as measured by anti-mouse soluble cotinine ELISA. Key respiratory parameters were assessed in age-matching cigarette smoke- and room air-exposed knockouts and wild-type mice and the averages of three maneuvers per mouse are shown, along with the age group mean. (C) Pressure-volume (PV) loops (red solid line, cigarette smoke-exposed knockouts, n = 7; red dashed line, room air-exposed knockouts, n = 7; gray dashed line, room air-exposed wild type, n = 5; gray solid line, cigarette smoke-exposed wild type, n = 8). (D) Static compliance and (E) tissue elastance are shown. Histological changes were assessed in fixed lung sections. (F–H) Representative segmented images of left lung lobe showing airway and alveolar boundaries (black contour line) (cigarette smoke-exposed wild-type control [F], cigarette smoke-exposed knockouts [G], and age-matched room air-exposed knockouts [H]) (see also [Materials and methods](#)). (I) Histogram of distribution, showing remarkably decreased probability density in the healthy alveolar diameter range (20–40 µm) and increased probability density in the damaged range (50–80 µm) in 18-week-old cigarette smoke-exposed knockout mice (white bar outlined in red, n = 8) compared with room air-exposed knockout control (red bar, n = 5). (J) No change in alveolar diameter (legend continued on next page)

non-genetic emphysema. As detailed in our previous publication, three lines of quintuple *Serpina1a-e* gene knockout mice were generated (A, B, and C), and the first two (A and B) were characterized. The difference between the three lines is at the DNA *serpinA1* locus level. While all three lines have the same phenotype, resulting from complete absence of circulating AAT, the resulting gene editing events for how each of the genes was disrupted were unique among the three lines.³⁹ Therefore, we used mouse line C, which was not characterized earlier, and confirmed that the line C phenotype is consistent with those of line A and line B.

Here, we expanded on the prior work and implemented a cigarette smoke exposure protocol, which accelerated the decline in lung function in *Serpina1a-e* knockout mice, while wild-type mice were not affected. We demonstrated that in the absence of functional AAT, cigarette smoke induced aggravated destruction of alveolar walls and changes in the lung mechanical behavior associated with loss of lung tissue elastic recoil. These findings parallel clear evidence that for individuals with AATD, smoking is a major risk factor for lung disease. Emphysema in smokers is associated with greater chronic expiratory airflow obstruction, increased rate of airflow decline over time, younger age of disease onset, and overall shorter life expectancy.⁴⁰

The primary objective of this study was to test the efficacy of rAAV-mediated human *SERPINA1* gene constructs for liver-directed therapy of slowly progressing and accelerated pulmonary emphysema in *Serpina1a-e* knockout mice. We tested the efficacy of the two AAV vectors for human *SERPINA1* gene delivery and hAAT protein expression by hepatocytes using AAT null mice. We did not intend to compare the potency or the efficacy of the two constructs. While the single-function vector was designed to deliver wild-type hAAT M, the dual-function vector construct was designed to deliver hAAT M Ala213. The latter naturally occurring variant represents an amino acid substitution in the AAT M protein at 213, of Val to Ala, which is overrepresented in patients with the PiZ mutation. This variant has no apparent effect on the function or metabolism of the protein and it is functionally identical to wild-type hAAT M.⁴¹

Treatment with rAAV generated dose-dependent systemic levels of hAAT protein that rise significantly above the serum protective threshold level of 572 $\mu\text{g}/\text{mL}$ (11 μM). In particular, the levels up to 10,000 $\mu\text{g}/\text{mL}$ (>2,000 μM) at a dose of 2.9×10^{11} gc per animal are 10 to 5 times the normal human levels estimated to be 1,000 to 2,000 $\mu\text{g}/\text{mL}$ (20–53 μM). Measurements of the biological activity of hAAT against human neutrophil elastase indicated that the liver secreted biochemically active hAAT, which could inhibit neutrophil elastase. Transgene levels were sufficient to restore the protease-anti-

protease balance and halt the irreversible degradation of elastin that provides resilience and elasticity to the lung tissue. Decreased lung compliance and increased elastic recoil indicate that mice treated with rAAV-hAAT largely conserved the elastic properties of their lung tissue compared with vehicle-treated controls. Remarkably, a significant presence of neutrophils in lung airways correlated with progression of emphysema in both the spontaneous and the cigarette smoke exposure models, supporting the idea that neutrophil recruitment plays a role in this mouse model, as it does in humans. We also observed increased presence of lymphocytes in both knockout and wild-type mice enrolled in the longitudinal study. One possible hypothesis is aging. This age-related increased influx of lymphocytes would be supported by the literature in both humans and mice.^{42,43} Given the data provided here and from several earlier studies, we can now conclude that alveolar destruction is driven largely by increased levels of elastase activity derived from activated neutrophils.^{13,16,21,39,44,45} In summary, we propose the *Serpina1a-e* knockout mouse as a model of genetic and cigarette smoke-induced emphysema; we further provide evidence that rAAV-mediated gene therapy can compensate for the loss-of-function disease and restore protease-antiprotease balance and ultimately prevent development of or slow down the progression of *SERPINA1*-associated lung disease. Restoration of the protease-antiprotease balance may also lead to more successful outcomes of regenerative therapy for AATD patients at different stages of emphysema.^{46–49} Gene therapy for AATD is still in the initial phases of development for humans. Although promising, the first trials have not given satisfactory results so far, due to the low serum levels of AAT achieved and the frequent development of immune response against viral vector.^{50–55}

Overall, the research presented here demonstrates the efficacy of systemic liver-directed gene augmentation therapy in the first animal model of AATD. Importantly, basing efficacy on functional readouts, as opposed to serum level quantification, may help in the development of more efficacious treatments for patients with AATD.

Although we provided considerable empirical results to support the effectiveness of the liver-directed gene augmentation therapy, there are two major limitations in this study that will be addressed in our future research. First, the study is focused on hAAT activity against its primary target, neutrophil elastase. However, AAT also demonstrates protease inhibitory activity against other proteases, in particular the proteinase 3 (PR3). We have no evidence that hAAT is also inhibiting mouse PR3, which could potentially explain why AAV treatments do not precisely mimic the mouse wild-type phenotype. Second, obtaining the evidence of increased levels and antiproteases activity of hAAT in the mouse lung epithelial lining would add to the value of the findings and solidify the concept. These

distribution was observed in wild-type mice (gray bar, room air, n = 4; white bar outlined in black, smoke, n = 9). A dramatic shift in PV loops upward (in C), increased compliance (in D), and decreased tissue elastance (in E) are due to cigarette smoke-induced destruction of the alveolar walls (in G) resulting in overinflation of the lung, which become evident as early as 18 weeks of age in cigarette smoke-exposed knockout mice, while wild-type mice tolerated (in C, D, and F) the cigarette smoking regimen well. Error bars represent the SEM. Statistical significance was determined by two-tailed unpaired t test, except for the PV loops (two-way ANOVA). ns, p > 0.05; *p ≤ 0.05; **p ≤ 0.01; ***p ≤ 0.001; ****p ≤ 0.0001. Scale bars, 1 mm (top), 150 μm (bottom).

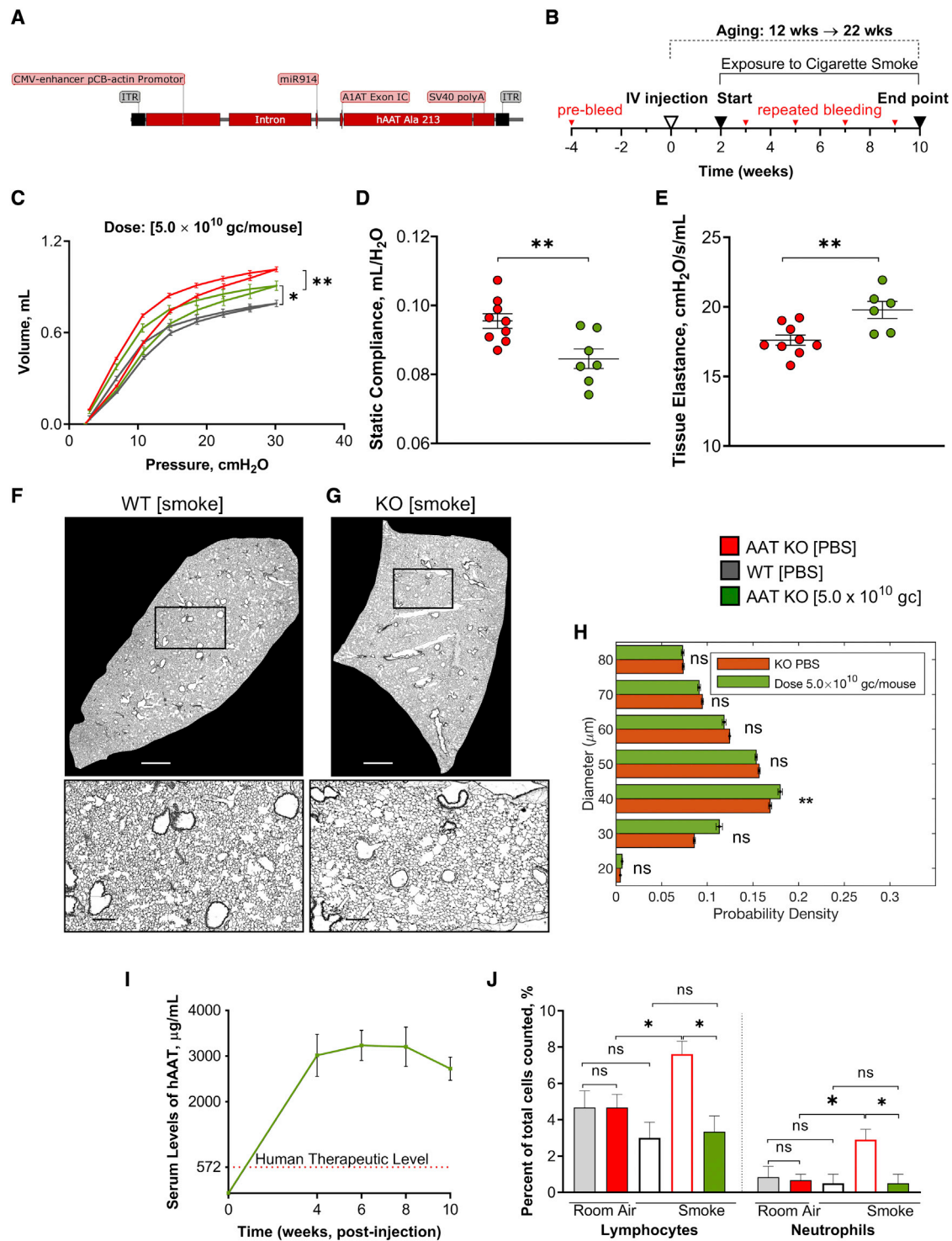


Figure 5. rAAV-mediated *SERPINA1* transgene expression protects lung parenchyma and preserves pulmonary function in *Serpina1a-e* knockout mice exposed to cigarette smoke

(A) Schematic of the dual-function (df.CB-hAAT) vector construct. The expression cassettes contain a single-stranded DNA molecule with AAV serotype 2 inverted terminal repeats (ITRs) flanking a gene cassette comprising cytomegalovirus immediate-early enhancer/chicken β -actin hybrid promoter sequences, cDNA encoding wild-type human α_1 -antitrypsin (AAT) protein with exon 1C, and an SV40 polyadenylation signal. The recombinant dual-function construct is assembled by inserting a gene-silencing

(legend continued on next page)

measurements can be made using bronchoalveolar lavage fluid and the same analytical methods that were used here for serum samples.

It is well understood that preclinical animal models not only are the key to understanding the pathophysiology of a disease, but also are crucial for selecting the correct therapeutic approach. To study major aspects of human disease associated with AATD, an ideal murine mouse model should have no mouse AAT expression and a single copy of human PiZ inserted in the specific locus of the DNA sequence on a mouse chromosome. However, each animal model has its pros and cons, and selection of one depends on the nature of the study to be conducted.

In this study we are focused on the respiratory disease phenotype and integrity of lung parenchyma. We tested AAV vectors as tools for human M-AAT expression as well as the functionality of the protein produced. The AAT knockout mouse model of genetic emphysema not only provides excellent information on the development of emphysema and the associated disease progression respiratory insufficiency, but also allows us to test a new strategy for the AATD gene therapy.

Translating these exciting data into larger species will likely be challenging, as evidenced by the difficulties several sponsors faced in the past in trying to reach high enough serum levels in patients. While the minimal therapeutic level with a stably expressed gene product may be lower than a protein replacement product, where the pharmacokinetics has large swings between peak and trough, this has not yet been determined. We believe that future studies in these mice will allow for that evaluation as well as a head-to-head comparison of different therapeutic modalities for their effectiveness at halting the progression of AATD lung disease.

MATERIALS AND METHODS

Animals

All experimental procedures were approved by the Institutional Animal Care and Use Committee at the University of Massachusetts

Medical School. Quintuple *Serpina1a-e* gene knockout (B6.129Serpina1a-e^{em5UMMS}) (also called as line 31C)³⁹ and wild-type C57BL/6J mice were housed in groups of five on a 12-h light cycle and had free access to water, were fed a standard mouse chow *ad libitum*, and were bred in-house. Adult male mice were used in all studies. *Serpina1a-e* knockout mice and wild-type controls were enrolled in the cross-sectional study at the age of 18 weeks (n = 10), 28 weeks (n = 10), or 52 weeks (n = 12). *Serpina1a-e* knockout mice and wild-type controls were enrolled in the cigarette smoke-aggravated emphysema study at 10 weeks of age (n = 16 per strain). *Serpina1a-e* knockout mice were randomly assigned to one of the four treatment groups: (1) AAV8.df-AAT (n = 24) or (2) vehicle (phosphate-buffered saline [PBS]) (n = 12) at the age of 12 weeks (enrolled in the attenuation of cigarette smoke-induced emphysema study), or (3) AAV8.AAT (n = 24) or (4) vehicle (PBS) (n = 10) at the age of 16 weeks (enrolled in the prevention of spontaneous emphysema study). In addition, wild-type control mice (n = 8) were enrolled in the attenuation of cigarette smoke-induced emphysema study at the age of 22 weeks. To evaluate cigarette smoking status, *Serpina1a-e* knockout (n = 5) and wild-type (n = 5) mice were used for the measurement of cotinine in mouse serum at the age of 28 weeks.

Recombinant AAV vectors

The rAAV serotype 8 vectors used in this study were generated, purified, and titered at the University of Massachusetts Gene Therapy Vector Core as previously described.⁵⁶ The vector constructs contain a single-stranded DNA molecule with AAV serotype 2 inverted terminal repeats flanking a gene cassette comprising cytomegalovirus immediate-early enhancer/chicken β -actin hybrid promoter sequences, wild-type exon 1C, cDNA encoding either wild-type (M allele) hAAT in single-function vector or the sequence of the hAAT M allele with alanine 213 (MAla213) in a dual-function vector and an SV40 polyadenylation signal.²⁹ The recombinant dual-function construct is assembled by inserting a gene-silencing artificial miR914 before the start codon of the hAAT transgene as described

artificial miR914 before the start codon of the human AAT transgene. The expression cassette was packaged in the liver-specific rAAV serotype 8 capsid. (B) Schematic showing the experimental design: the rAAV-hAAT dual-function vector was systemically infused by a single tail vein injection at 5.0×10^{10} gc/mouse into the livers of 12-week-old knockout mice, and the mice were exposed to cigarette smoke 2 weeks later for a period of 8 weeks. Mouse serum was collected to measure human AAT at various time points (red triangles) (see also [Materials and methods](#)). Key respiratory parameters were assessed in age-matched cigarette smoke-exposed knockouts and wild-type mice, and the averages of three maneuvers per mouse are shown, along with the age group mean. (C) Pressure-volume (PV) loops (red line, vehicle-treated knockout control, n = 9; green line, rAAV-treated knockouts, n = 7; gray line, wild-type control, n = 8). (D) Static compliance and (E) tissue elastance are shown. Histological changes were assessed in fixed lung sections. (F and G) Representative segmented images of left lung lobe showing airway and alveolar boundaries (black contour line) (cigarette smoke-exposed wild-type mice (F, top and bottom) and knockout mice treated with rAAV at 5.0×10^{10} gc (G, top and bottom) (see [Materials and methods](#)). (H) Histogram of distribution, showing increased probability density in the healthy alveolar diameter range (20–40 μ m) and evenly distributed probability density in the damaged range (50–80 μ m) in human AAT transgene-expressing cigarette smoke-exposed knockout mice (green bar, n = 6) compared with vehicle-treated knockout control (red bar, n = 4). Shift of PV loops downward (in C), decreased lung compliance (in D), and increased elastic recoil (in E) indicate that mice expressing wild-type human AAT protease inhibitor protein were protected from cigarette smoke and largely preserve the elastic properties of the lung tissue and the integrity of the interalveolar septa compared with vehicle-treated control knockout mice. (I) Dual-function vector generated sufficiently high-level transgene expression to produce significant systemic levels of human AAT protein (green line, $\sim 3,000$ μ g/mL at the endpoint, n = 3), as measured by ELISA. (J) Cellular analysis of bronchoalveolar lavage cytopins reflects increased inflammatory cell profiles in cigarette smoke-exposed vehicle-treated control knockout mice (gray bar, wild-type room air-exposed control; red bar, room air-exposed knockout control; white outlined in black bar, cigarette smoke-exposed wild type; white outlined in red bar, cigarette smoke-exposed knockout; green bar, rAAV-treated cigarette smoke-exposed knockout; n = 3 per group). Lymphocyte (left) and neutrophil (right) counts are significantly reduced in cigarette smoke-exposed rAAV-treated mice compared with cigarette smoke-exposed vehicle-treated knockout mice and are comparable to those of cigarette smoke-exposed wild-type mice. Error bars represent the SEM. Statistical significance was determined by two-tailed unpaired t test or the Holm-Sidak method (cell counting), with $\alpha = 0.05$, except for the PV loops (two-way ANOVA). ns, p > 0.05; *p \leq 0.05; **p \leq 0.01. Scale bars, 1 mm (top), 200 μ m (bottom).

earlier.⁵⁷ Final formulations of dual-function AAV8.df-CB-AAT used in the accelerated cigarette smoke-induced emphysema study and single-function AAV8.CB-AAT vector used in the longitudinal spontaneous emphysema study were in PBS. All viral vector doses were per animal, at 2.9×10^{11} , 1.4×10^{11} , 5.0×10^{10} , or 5.0×10^9 gc or vehicle. Animals received a single intravenous injection in a total volume of 200 μ L (or PBS for vehicle group) into the tail vein.

Measurements of pulmonary mechanics

Invasive lung function measurements were performed at the study endpoint using the forced oscillation technique (flexiVent FX1 system, SCIREQ, Montreal, QC, Canada), broadly acknowledged as the gold standard for pulmonary function tests in mice.

Animals were anesthetized with an intraperitoneal (i.p.) injection of a mixture of ketamine hydroxylchloride (90 mg/kg, Patterson Veterinary, product 07-890-8598, Greeley, CO), or ketaset (90 mg/kg, Fort Dodge Animal Health, product 0856-2013-01, Fort Dodge, IA) and xylazine (4.5 mg/kg, Lloyd, product 343720RX, Santa Cruz Animal Health, Dallas, TX), or rompun (4.5 mg/kg, Bayer, product 321350RX, Leverkusen, Germany) to maintain a surgical plane of anesthesia during the entire procedure. The anesthetized mouse was placed in a supine position on a heating pad during the course of the tracheotomy. The surgical area was cleaned with 70% alcohol, and a 2- to 3-cm skin incision was made directly over the trachea, the underlying fat pads were reflected laterally, and the sternohyoid and omohyoid muscles were separated over the trachea with blunt dissection. To secure a cannula in place, the trachea was exposed a few millimeters caudal to the larynx and a surgical silk thread was passed under the trachea using fine curved-tip forceps and then the thread was tied into a single knot around tubing in the trachea.

A partial incision was then made between the tracheal cartilage rings followed by insertion of a precalibrated 18G cannula into the trachea. The flexiVent machine was turned on at this point, and a default ventilation profile was used. The mouse was then connected to the ventilator via the Y-tubing. The cannulated animal was aligned to the ventilator to avoid a possible cannula occlusion or tracheal twist. To ensure proper placement once the mouse is ventilated, a deep inflation was administered to ensure bilateral chest rise. In addition, during the deep inflation, a pressure of 30 cmH₂O over a 3-s period was applied, and this also ensures the absence of a leak. Once adequate cannulated animal placement was confirmed, a mechanical scan was performed to measure baseline pulmonary mechanics. The flexiVent system can provide mechanical ventilatory support with control of tidal volumes, pulmonary pressures (inspiratory and expiratory pressures), respiratory rate, and oxygen flow. Spontaneous respiratory effort was prevented using a neuromuscular blocking agent (pancuronium bromide, 0.2 mg/kg; Hospira, product 00409464601, Lake Forest, IL, or rocuronium bromide, 0.6 mg/kg; X-Gen Pharmaceuticals, product 1006740, Horseheads, NY). Respiratory mechanics were obtained and calculated using flexiWare v.8.2v software (flexiVent system, SCIREQ, Montreal, QC, Canada) as previously described.⁵⁸ Once the experiment was completed, the ventilation was stopped,

and the cannulated mouse was detached from the flexiVent and then euthanized by cervical dislocation followed by a bilateral thoracotomy. At the endpoint of each study, the raw data were collected for 3 consecutive days with the measurements of at least two control animals on every day of the experiments. The measurements were consequently repeated three times for each mouse (referred to as “three maneuvers per mouse”) and the average of the corresponding parameters was then considered. To characterize the disease model and evaluate the effect of the therapeutic approach, the key respiratory parameters were then analyzed. In particular, the pressure-volume loops assess the intrinsic elastic properties of the respiratory system and describe the mechanical behavior of the lungs and chest wall during inflation and deflation. The inflation (lower arm) and deflation (upper arm) arms differ at any given pressure. Due to destruction of the alveolar wall resulting in the loss of the lung parenchyma elastic recoil, the lower pressure is needed to inflate emphysematous lungs to a higher volume. Pressure-volume loops are a must in our research, where a change in elasticity is expected. Static compliance is the classic parameter extracted from a pressure-volume curve. It reflects the intrinsic elastic properties of the respiratory system. Compliance refers to the ability of the lungs to stretch and expand. Compliance can be calculated by dividing volume by pressure. It is increasing as emphysema is progressing. Tissue elastance describes an index of tissue stiffness. It represents the elastic energy stored within the tissue following the imposed deformation and therefore the ability of the tissue to retract and revert to its original shape. Elastance is the reciprocal of compliance and vice versa. Tissue elastance is decreased in emphysema due to diminished cellular elastic properties.^{58,59}

Histology and morphometry

Immediately following the measurements of pulmonary functions (flexiVent), bronchoalveolar lavage (BAL) fluid was collected or lungs were harvested to quantify alveolar air spaces to further characterize emphysema progression in every experimental group. To collect airway cells, lungs were slowly inflated via cannula with 1 mL cold PBS using a 3-mL syringe. Collected cells were spun down at 1,500 rpm for 5 min and supernatant was separated and stored at -80° C. The cell pellet was resuspended in 500 μ L PBS. Cell aliquots of 50 μ L were mixed with 50 μ L of 0.4% trypan blue (Thermo Fisher Scientific, product 15250061, Waltham, MA) and total cell count was performed using a Hausser Bright-Line Phase hemacytometer (Horsham, PA). To prepare cell cytopspins, 200 μ L of the cell suspension was used. BAL cells were spun onto labeled glass slides at 500 rpm for 10 min (Shandon Cytospin 3 centrifuge, Nottingham, UK). Air-dried slides were stained using a Kwik-Diff stain kit (Fisher Scientific Shandon Kwik-Diff stain kit, product 9990700, Waltham, MA). The stained BAL cells were imaged, and differential cell count was performed using ImageJ1.x software.⁶⁰ Per cytopspin, 200 cells were counted for the absolute number of lymphocytes, neutrophils, and macrophages, differentiated by standard morphology and staining characteristics. Prior to collection of the lung tissue for histopathology, the lung vascular bed was perfused using a 10-mL syringe filled with 5 mL PBS. A small incision in the left ventricle was made to connect a 21G needle and the needle was inserted into the right ventricle.

The lung histopathology was performed on the lungs fixed with phosphate buffered 10% formalin (Fisher Scientific, 6764240, Waltham, MA). The lungs were fixed at a constant hydrostatic pressure of a 25-cm formalin column for at least 5 min and post-fixed in formalin. The lung lobes were separated and embedded in paraffin using a routine procedure. Three 3- μ m-thick sections were obtained at a distance of 100 μ m from one another and were stained with hematoxylin and eosin. Three sections per mouse left lung lobe were tile scanned using a Leica DM5500B upright microscope and resized with Leica LAS X software. Image backgrounds were made black with a brush tool using Adobe Photoshop CS4 software. To obtain values of the air-space diameters, tile scans of equal pixel size were further segmented to locate alveolar boundaries using a previously published MATLAB (MathWorks, Natick, MA) program.^{61,62} The relationship between a range of air-space diameters and their probability (that is, “probability density”) as well as statistics were analyzed using MATLAB scripts (MathWorks, Natick, MA).

Cigarette smoke exposure

A reference cigarette, the 3R4F type (developed in the Cigarette Laboratory at the Tobacco and Health Research Institute, University of Kentucky, Lexington, KY), with machine cigarette smoking regimens defined by the International Organization for Standardization (ISO) was used. Animals were exposed to cigarette smoke via a computer-controlled smoke exposure configuration apparatus in a whole-body chamber (inExpose system, SCIREQ, Montreal, QC, Canada). Test mice were exposed to the ISO standard puffing profile with mainstream cigarette smoke. Each cigarette was 35 mL puff volume, 2 s puff duration, 7 puffs per cigarette, and frequency of 1 puff per minute. In phase 1, mice of each strain were exposed to two 3R4F cigarettes 5 days a week for 2 weeks. Phase 2 followed as four 3R4F cigarettes twice per day, 5 days a week, for an additional 6 weeks. Control animals were exposed to room air.

ELISA

rAAV-treated mice were bled via the facial vein in the first 2 months biweekly and then monthly. To measure levels of hAAT in the mouse serum, an hAAT ELISA kit from GenWay (product GWB-5428A0, San Diego, CA) was used per the manufacturer protocol. A cotinine (mouse/rat) ELISA kit (Abnova, product KA2264, Walnut, CA) was used per the manufacturer protocol for the measurements of cotinine levels in mouse serum collected within 1 h of cigarette smoking cessation. The human neutrophil elastase activity assay was from Enzo Life Sciences (product BML-AK497-0001, Farmingdale, NY). All plates were analyzed using SoftMax Pro 4.8 software.

Statistics

Statistical analyses were performed using GraphPad Prism v.7 (GraphPad, La Jolla, CA) or MATLAB (MathWorks, Natick, MA). Statistical significance was determined by two-way ANOVA for measures of pressure-volume loops in respiratory mechanics, by the Holm-Sidak method for cell counting, with $\alpha = 0.05$, or by two-tailed unpaired t test. Significance was considered to be at $p < 0.05$ with 95% confidence level.

SUPPLEMENTAL INFORMATION

Supplemental information can be found online at <https://doi.org/10.1016/j.omtm.2022.04.003>.

ACKNOWLEDGMENTS

This work was supported by the Alpha-1 Foundation and a National Institutes of Health grant (PO1H2131471). The graphical abstract was created with [BioRender.com](https://www.biorender.com). We would like to thank our colleagues at the Department of Animal Medicine at the University of Massachusetts Chan Medical School, for helping us with cigarette smoke exposure studies, and to acknowledge Guangping Gao, Alisha Gruntman, Claudio Punzo, Yu Liu, and Jayme Heywosz for services provided at the University of Massachusetts Chan Medical School Viral Vector Core, Respiratory Core, Microscopy Core and Morphology Core, respectively.

AUTHOR CONTRIBUTIONS

M.Z. designed the study; conducted experiments; acquired, analyzed, and interpreted data; generated figures; and wrote the manuscript. F.B. conceptualized the study, interpreted data, and wrote the manuscript. C.G. conducted experiments; G.G. helped design vector constructs; M.B. helped generate vector plasmids; T.R.F. acquired funding and provided clinical context for interpretation of animal models; and C.M. acquired funding, conceptualized the study, designed vector constructs, and analyzed and interpreted data.

DECLARATION OF INTERESTS

T.R.F. is a scientific advisor to Ferring Ventures, S.A.

REFERENCES

- Strange, C. (2020). Alpha-1 antitrypsin deficiency associated COPD. *Clin. Chest Med.* 41, 339–345.
- Cazzola, M., Stolz, D., Rogliani, P., and Matera, M.G. (2020). α 1-Antitrypsin deficiency and chronic respiratory disorders. *Eur. Respir. Rev.* 29, 190073.
- Lomas, D.A. (2018). New therapeutic targets for alpha-1 antitrypsin deficiency. *Chronic Obstr. Pulm. Dis.* 5, 233–243.
- Larsson, C. (1978). Natural history and life expectancy in severe alpha1-antitrypsin deficiency. *Pi Z. Acta Med. Scand.* 204, 345–351.
- de Serres, F.J., and Blanco, I. (2012). Prevalence of α 1-antitrypsin deficiency alleles PI*S and PI*Z worldwide and effective screening for each of the five phenotypic classes PI*MS, PI*MZ, PI*SS, PI*SZ, and PI*ZZ: a comprehensive review. *Ther. Adv. Respir. Dis.* 6, 277–295.
- Craig, T.J., and Henaou, M.P. (2018). Advances in managing COPD related to α (1)-antitrypsin deficiency: an under-recognized genetic disorder. *Allergy* 73, 2110–2121.
- Stoller, J.K., and Aboussouan, L.S. (2012). A review of α 1-antitrypsin deficiency. *Am. J. Respir. Crit. Care Med.* 185, 246–259.
- Bornhorst, J.A., Greene, D.N., Ashwood, E.R., and Grenache, D.G. (2013). α 1-Antitrypsin phenotypes and associated serum protein concentrations in a large clinical population. *Chest* 143, 1000–1008.
- de Serres, F., and Blanco, I. (2014). Role of alpha-1 antitrypsin in human health and disease. *J. Intern. Med.* 276, 311–335.
- Stoller, J.K., and Aboussouan, L.S. (2005). Alpha1-antitrypsin deficiency. *Lancet* 365, 2225–2236.
- Laurell, C.-B. (1971). Is emphysema in AlphasAntitrypsin deficiency a result of auto-digestion? *Scand. J. Clin. Lab. Invest.* 28, 1–3.

12. Kawabata, K., Hagio, T., and Matsuoka, S. (2002). The role of neutrophil elastase in acute lung injury. *Eur. J. Pharmacol.* *451*, 1–10.
13. Guyot, N., Wartelle, J., Malleret, L., Todorov, A.A., Devouassoux, G., Pacheco, Y., Jenne, D.E., and Belaouaj, A. (2014). Unopposed cathepsin G, neutrophil elastase, and proteinase 3 cause severe lung damage and emphysema. *Am. J. Pathol.* *184*, 2197–2210.
14. Rønnow, S.R., Langholm, L.L., Sand, J.M.B., Thorlacius-Ussing, J., Leeming, D.J., Manon-Jensen, T., Tal-Singer, R., Miller, B.E., Karsdal, M.A., and Vestbo, J. (2019). Specific elastin degradation products are associated with poor outcome in the ECLIPSE COPD cohort. *Sci. Rep.* *9*, 4064.
15. Sinden, N.J., and Stockley, R.A. (2013). Proteinase 3 activity in sputum from subjects with alpha-1-antitrypsin deficiency and COPD. *Eur. Respir. J.* *41*, 1042–1050.
16. Newby, P.R., Crossley, D., Crisford, H., Stockley, J.A., Mumford, R.A., Carter, R.I., Bolton, C.E., Hopkinson, N.S., Mahadeva, R., Steiner, M.C., et al. (2019). A specific proteinase 3 activity footprint in α 1-antitrypsin deficiency. *ERJ Open Res.* *5*, 00095-02019.
17. Korkmaz, B., Moreau, T., and Gauthier, F. (2008). Neutrophil elastase, proteinase 3 and cathepsin G: physicochemical properties, activity and physiopathological functions. *Biochimie* *90*, 227–242.
18. Petrache, I., Fijalkowska, I., Medler, T.R., Skirball, J., Cruz, P., Zhen, L., Petrache, H.I., Flotte, T.R., and Tuder, R.M. (2006). alpha-1 antitrypsin inhibits caspase-3 activity, preventing lung endothelial cell apoptosis. *Am. J. Pathol.* *169*, 1155–1166.
19. Lockett, A.D., Van Demark, M., Gu, Y., Schweitzer, K.S., Sigua, N., Kamocki, K., Fijalkowska, I., Garrison, J., Fisher, A.J., Serban, K., et al. (2012). Effect of cigarette smoke exposure and structural modifications on the α -1 Antitrypsin interaction with caspases. *Mol. Med.* *18*, 445–454.
20. Stockley, R.A. (2015). The multiple facets of alpha-1-antitrypsin. *Ann. Transl. Med.* *3*, 130.
21. Janciauskiene, S., Wrenger, S., Immenschuh, S., Olejnicka, B., Greulich, T., Welte, T., and Chorostowska-Wynimko, J. (2018). The multifaceted effects of alpha-1-antitrypsin on neutrophil functions. *Front. Pharmacol.* *9*, 341.
22. Gadek, J.E., Fells, G.A., Zimmerman, R.L., Rennard, S.I., and Crystal, R.G. (1981). Antielastases of the human alveolar structures. Implications for the protease-antiprotease theory of emphysema. *J. Clin. Invest.* *68*, 889–898.
23. Gadek, J.E., Fells, G.A., and Crystal, R.G. (1979). Cigarette smoking induces functional antiprotease deficiency in the lower respiratory tract of humans. *Science* *206*, 1315–1316.
24. Brantly, M.L., Paul, L.D., Miller, B.H., Falk, R.T., Wu, M., and Crystal, R.G. (1988). Clinical features and history of the destructive lung disease associated with alpha-1-antitrypsin deficiency of adults with pulmonary symptoms. *Am. Rev. Respir. Dis.* *138*, 327–336.
25. McElvaney, N.G., Burdon, J., Holmes, M., Glanville, A., Wark, P.A.B., Thompson, P.J., Hernandez, P., Chlumsky, J., Teschler, H., Ficker, J.H., et al. (2017). Long-term efficacy and safety of alphas proteinase inhibitor treatment for emphysema caused by severe alpha1 antitrypsin deficiency: an open-label extension trial (RAPID-OLE). *Lancet Respir. Med.* *5*, 51–60.
26. Chiuchiolio, M.J., and Crystal, R.G. (2016). Gene therapy for alpha-1 antitrypsin deficiency lung disease. *Ann. Am. Thorac. Soc.* *13*, S352–S369.
27. Lorincz, R., and Curiel, D.T. (2020). Advances in alpha-1 antitrypsin gene therapy. *Am. J. Respir. Cell Mol. Biol.* *63*, 560–570.
28. Conlon, T.J., Cossette, T., Erger, K., Choi, Y.-K., Clarke, T., Scott-Jorgensen, M., Song, S., Campbell-Thompson, M., Crawford, J., and Flotte, T.R. (2005). Efficient hepatic delivery and expression from a recombinant adeno-associated virus 8 pseudotyped α 1-antitrypsin vector. *Mol. Ther.* *12*, 867–875.
29. Song, S., Embury, J., Laipis, P.J., Berns, K.I., Crawford, J.M., and Flotte, T.R. (2001). Stable therapeutic serum levels of human alpha-1 antitrypsin (AAT) after portal vein injection of recombinant adeno-associated virus (rAAV) vectors. *Gene Ther.* *8*, 1299–1306.
30. Xiao, W., Berta, S.C., Lu, M.M., Moscioni, A.D., Tazelaar, J., and Wilson, J.M. (1998). Adeno-associated virus as a vector for liver-directed gene therapy. *J. Virol.* *72*, 10222–10226.
31. Mueller, C., Gernoux, G., Gruntman, A.M., Borel, F., Reeves, E.P., Calcedo, R., Rouhani, F.N., Yachnis, A., Humphries, M., Campbell-Thompson, M., et al. (2017). 5 Year expression and neutrophil defect repair after gene therapy in alpha-1 antitrypsin deficiency. *Mol. Ther.* *25*, 1387–1394.
32. Song, S., Morgan, M., Ellis, T., Poirier, A., Chesnut, K., Wang, J., Brantly, M., Muzyczka, N., Byrne, B.J., Atkinson, M., et al. (1998). Sustained secretion of human alpha-1-antitrypsin from murine muscle transduced with adeno-associated virus vectors. *Proc. Natl. Acad. Sci. U S A* *95*, 14384–14388.
33. Chulay, J.D., Ye, G.-J., Thomas, D.L., Knop, D.R., Benson, J.M., Hutt, J.A., Wang, G., Humphries, M., and Flotte, T.R. (2010). Preclinical evaluation of a recombinant adeno-associated virus vector expressing human alpha-1 antitrypsin made using a recombinant herpes simplex virus production method. *Hum. Gene Ther.* *22*, 155–165.
34. De, B., Heguy, A., Leopold, P.L., Wasif, N., Korst, R.J., Hackett, N.R., and Crystal, R.G. (2004). Intraleural administration of a serotype 5 adeno-associated virus coding for alpha1-antitrypsin mediates persistent, high lung and serum levels of alpha1-antitrypsin. *Mol. Ther.* *10*, 1003–1010.
35. Chiuchiolio, M.J., Kaminsky, S.M., Sondhi, D., Hackett, N.R., Rosenberg, J.B., Frenk, E.Z., Hwang, Y., Van de Graaf, B.G., Hutt, J.A., Wang, G., et al. (2013). Intraleural administration of an AAVrh.10 vector coding for human α 1-antitrypsin for the treatment of α 1-antitrypsin deficiency. *Hum. Gene Ther. Clin. Dev.* *24*, 161–173.
36. Halbert, C.L., Madtes, D.K., Vaughan, A.E., Wang, Z., Storb, R., Tapscott, S.J., and Miller, A.D. (2010). Expression of human alpha1-antitrypsin in mice and dogs following AAV6 vector-mediated gene transfer to the lungs. *Mol. Ther.* *18*, 1165–1172.
37. De, B.P., Heguy, A., Hackett, N.R., Ferris, B., Leopold, P.L., Lee, J., Pierre, L., Gao, G., Wilson, J.M., and Crystal, R.G. (2006). High levels of persistent expression of alpha1-antitrypsin mediated by the nonhuman primate serotype rh.10 adeno-associated virus despite preexisting immunity to common human adeno-associated viruses. *Mol. Ther.* *13*, 67–76.
38. Fregonese, L., Stolk, J., Frants, R.R., and Veldhuisen, B. (2008). Alpha-1 antitrypsin Null mutations and severity of emphysema. *Respir. Med.* *102*, 876–884.
39. Borel, F., Sun, H., Zieger, M., Cox, A., Cardozo, B., Li, W., Oliveira, G., Davis, A., Gruntman, A., Flotte, T.R., et al. (2018). Editing out five Serpin1 paralogs to create a mouse model of genetic emphysema. *Proc. Natl. Acad. Sci. U S A* *115*, 2788–2793.
40. Needham, M., and Stockley, R.A. (2004). α 1-Antitrypsin deficiency. 3: clinical manifestations and natural history. *Thorax* *59*, 441–445.
41. Nukiwa, T., Brantly, M., Ogushi, F., Fells, G., Satoh, K., Stier, L., Courtney, M., and Crystal, R.G. (1987). Characterization of the M1(Ala213) type of .alpha.1-antitrypsin, a newly recognized, common “normal” .alpha.1-antitrypsin haplotype. *Biochemistry* *26*, 5259–5267.
42. Meyer, K., and Soergel, P. (1999). Variation of bronchoalveolar lymphocyte phenotypes with age in the physiologically normal human lung. *Thorax* *54*, 697–700.
43. Schulte, H., Mühlfeld, C., and Brandenberger, C. (2019). Age-related structural and functional changes in the mouse lung. *Front. Physiol.* *10*, 1466.
44. Genschmer, K.R., Russell, D.W., Lal, C., Szul, T., Bratcher, P.E., Noerager, B.D., Abdul Roda, M., Xu, X., Rezonzew, G., Viera, L., et al. (2019). Activated PMN exosomes: pathogenic entities causing matrix destruction and disease in the lung. *Cell* *176*, 113–126.e15.
45. Janoff, A., Raju, L., and Dearing, R. (1983). Levels of elastase activity in bronchoalveolar lavage fluids of healthy smokers and nonsmokers. *Am. Rev. Respir. Dis.* *127*, 540–544.
46. Kotton, D.N., and Morrisey, E.E. (2014). Lung regeneration: mechanisms, applications and emerging stem cell populations. *Nat. Med.* *20*, 822–832.
47. Akram, K.M., Patel, N., Spiteri, M.A., and Forsyth, N.R. (2016). Lung regeneration: endogenous and exogenous stem cell mediated therapeutic approaches. *Int. J. Mol. Sci.* *17*, 128.
48. Sun, Z., Li, F., Zhou, X., Chung, K.F., Wang, W., and Wang, J. (2018). Stem cell therapies for chronic obstructive pulmonary disease: current status of pre-clinical studies and clinical trials. *J. Thorac. Dis.* *10*, 1084–1098.
49. Weiss, D.J., Segal, K., Casaburi, R., Hayes, J., and Tashkin, D. (2021). Effect of mesenchymal stromal cell infusions on lung function in COPD patients with high CRP levels. *Respir. Res.* *22*, 142.

50. Brigham, K.L., Lane, K.B., Meyrick, B., Stecenko, A.A., Strack, S., Cannon, D.R., Caudill, M., and Canonico, A.E. (2000). Transfection of nasal mucosa with a normal alpha1-antitrypsin gene in alpha1-antitrypsin-deficient subjects: comparison with protein therapy. *Hum. Gene Ther.* *11*, 1023–1032.
51. Brantly, M.L., Spencer, L.T., Humphries, M., Conlon, T.J., Spencer, C.T., Poirier, A., Garlington, W., Baker, D., Song, S., Berns, K.I., et al. (2006). Phase I trial of intramuscular injection of a recombinant adeno-associated virus serotype 2 α 1-antitrypsin (AAT) vector in AAT-deficient adults. *Hum. Gene Ther.* *17*, 1177–1186.
52. Brantly, M.L., Chulay, J.D., Wang, L., Mueller, C., Humphries, M., Spencer, L.T., Rouhani, F., Conlon, T.J., Calcedo, R., Betts, M.R., et al. (2009). Sustained transgene expression despite T lymphocyte responses in a clinical trial of rAAV1-AAT gene therapy. *Proc. Natl. Acad. Sci. U S A* *106*, 16363–16368.
53. Mueller, C., Chulay, J.D., Trapnell, B.C., Humphries, M., Carey, B., Sandhaus, R.A., McElvaney, N.G., Messina, L., Tang, Q., Rouhani, F.N., et al. (2013). Human Treg responses allow sustained recombinant adeno-associated virus-mediated transgene expression. *J. Clin. Invest.* *123*, 5310–5318.
54. Mueller, C., and Flotte, T.R. (2013). Gene-based therapy for alpha-1 antitrypsin deficiency. *COPD* *10*, 44–49.
55. Flotte, T.R., Trapnell, B.C., Humphries, M., Carey, B., Calcedo, R., Rouhani, F., Campbell-Thompson, M., Yachnis, A.T., Sandhaus, R.A., McElvaney, N.G., et al. (2011). Phase 2 clinical trial of a recombinant adeno-associated viral vector expressing α 1-antitrypsin: interim results. *Hum. Gene Ther.* *22*, 1239–1247.
56. Gao, G.-P., Alvira, M.R., Wang, L., Calcedo, R., Johnston, J., and Wilson, J.M. (2002). Novel adeno-associated viruses from rhesus monkeys as vectors for human gene therapy. *Proc. Natl. Acad. Sci. U S A* *99*, 11854–11859.
57. Mueller, C., Tang, Q., Gruntman, A., Blomenkamp, K., Teckman, J., Song, L., Zamore, P.D., and Flotte, T.R. (2012). Sustained miRNA-mediated knockdown of mutant AAT with simultaneous augmentation of wild-type AAT has minimal effect on global liver miRNA profiles. *Mol. Ther.* *20*, 590–600.
58. McGovern, T.K., Robichaud, A., Fereydoonzad, L., Schuessler, T.F., and Martin, J.G. (2013). Evaluation of respiratory system mechanics in mice using the forced oscillation technique. *J. Vis. Exp.* e50172. <https://doi.org/10.3791/50172>.
59. Salazar, E., and Knowles, J.H. (1964). An analysis of pressure-volume characteristics of the lungs. *J. Appl. Physiol.* *19*, 97–104.
60. Schneider, C.A., Rasband, W.S., and Eliceiri, K.W. (2012). NIH Image to ImageJ: 25 years of image analysis. *Nat. Methods* *9*, 671–675.
61. Parameswaran, H., Majumdar, A., Ito, S., Alencar, A.M., and Suki, B. (2006). Quantitative characterization of airspace enlargement in emphysema. *J. Appl. Physiol.* *100*, 186–193.
62. Joshi, R., Heinz, A., Fan, Q., Guo, S., Monia, B., Schmelzer, C.E.H., Weiss, A.S., Batie, M., Parameswaran, H., and Varisco, B.M. (2018). Role for *Cela1* in postnatal lung remodeling and alpha-1 antitrypsin-deficient emphysema. *Am. J. Respir. Cell Mol. Biol.* *59*, 167–178.